The Filtered-x Least Mean Fourth Algorithm for Active Noise Cancellation and Its Convergence Behavior

Kang Seung Lee* *Regular Member*

ABSTRACT

In this paper, we propose the filtered-x least mean fourth (LMF) algorithm where the error raised to the power of four is minimized and analyze its convergence behavior for a multiple sinusoidal acoustic noise and Gaussian measurement noise. Application of the filtered-x LMF adaptive filter to active noise cancellation (ANC) requires estimating of the transfer characteristic of the acoustic path between the output and error signal of the adaptive controller. The results of the convergence analysis of the filtered-x LMF algorithm indicates that the effects of the parameter estimation inaccuracy on the convergence behavior of the algorithm are characterized by two distinct components : Phase estimation error and estimated gain. In particular, the convergence is shown to be strongly affected by the accuracy of the phase response estimate. Also, we newly show that convergence behavior can differ depending on the relative sizes of the Gaussian measurement noise and convergence constant.

I. Introduction

In active noise cancellation, the acoustic noise to be cancelled is often generated by rotating machines and thus can be modeled as the sum of a fundamental sinusoid and its harmonics. In this paper we are concerned with cancellation of fan noise based on ANC filtering. Fan noise is frequently generated in the consumer electronic products such as air conditioners, vacuum cleaners and so on. Adaptive approaches have widely been used in ANC applications in which the unwanted noise sound is adaptively synthesized with the equal amplitude but opposite phase, resulting in the cancellation of the acoustic noise as shown in Fig. 1[1~2]. In Fig. 1, the input microphone can be replaced by other non-acoustical sensors such as tachometers or accelerometers in which case the possibility of the speaker output feedback to the input microphone is removed. The adaptive filter output drives the loudspeaker in such a way that the acoustic noise and the loudspeaker output can be summed to null at the error microphone.

Although any adaptive algorithm can be used in Fig.1, the least mean square (LMS) algorithm has been the most popular one[3~5]. It has recently been found that the LMF algorithm in which the error raised to the power of four is minimized has better convergence properties[6~7]. It is noted, however, that the direct application of the LMS algorithm in Fig. 1 is not appropriate. The reason is that the acoustic path between the filter output and summation point of the error signal is frequency sensitive, which acts to distort the phase and magnitude of the error signal.

In turn, the distortion of the phase and magnitude in the error path can degrade the convergence performance of the LMS algorithm. As a result, the convergence rate is lowered, the residual error is increased, and the algorithm can even become unstable. For these reasons, it is necessary to use the so-called filtered-x LMS

* Dept. of Computer Engineering, DongEui University(kslee@dongeui.ac.kr)
논문번호 : K01198-0912, 접수일자 : 2001년 9월 12일
※ This paper was supported in part by 1999 post-doctorial program of Korea Science and Engineering Foundation(KOSEF) and 2001 research supporting program of DongEui University.

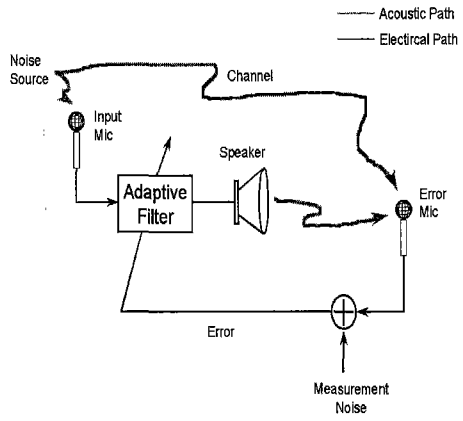

Fig. 1 Basic adaptive active noise canceller configuration.

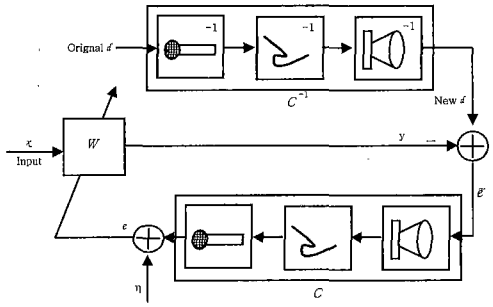

Fig. 2 Rearranged form of the canceller under linear system condition.

algorithm[8~12] for which the transfer characteristics between the output and the error signal of the adaptive canceller must be estimated.

In this paper, we propose a new filtered-x LMF algorithm for active cancellation of fan noise. It is noted that the fan noise can be modeled as the sum of a fundamental sinusoid and its harmonics. We first derive an adaptive canceller structure and then analyze its convergence behavior when the acoustic noise can be modeled as the sum of a fundamental sinusoid and its harmonics. The convergence analysis is focused on the effects of parameter estimation inaccuracy on the performance.

Following the introduction, we give a brief description of the underlying system model in Section Ⅱ. The results of the convergence analysis and the simulations are presented in Sections Ⅲ and Ⅳ, respectively. Finally we make a conclusions in Section Ⅴ.

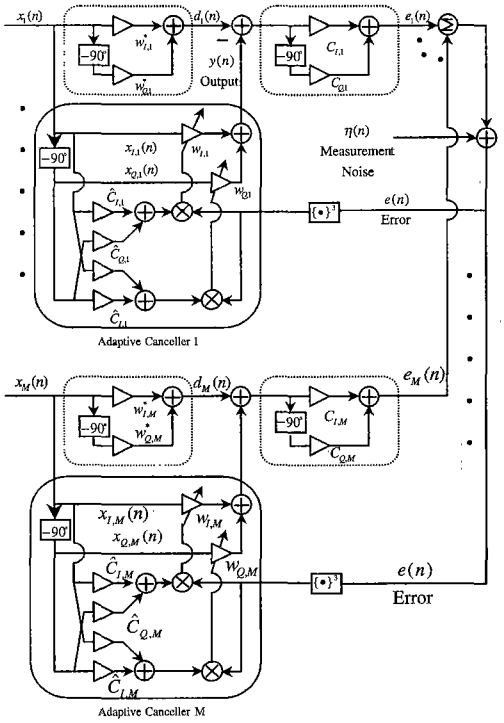

Fig. 3 The diagram of adaptive active noise canceller system under study.

Ⅱ. ANC System Model and Algorithm

Since the loudspeaker-air-microphone path of Fig. 1 is linear, one can easily get the equivalent system as shown in Fig. 2. When the noise consists of the multiple sinusoids, which is the case of fan noise, the acoustic and loudspeaker-acoustic-microphone can be described by the multiple in-phase (I) and quadrature (Q) weights as shown in the upper branch of Fig. 3.

For the m-th sinusoidal noise, the adaptive canceller structure also becomes to have two weights $\omega_{I,m}(n)$ and $\omega_{Q,m}(n)$, with I and Q inputs, $x_{I,m}(n)$ and $x_{Q,m}(n)$, respectively. Thus the output of the m-th canceller, $y_m(n)$ is expressed as

$$y_m(n) = \{ w_{I,m}(n)\, x_{I,m}(n) + x_{Q,m}(n)\, w_{Q,m}(n) \} \quad (1)$$

where

$$x_{I,m}(n) = A_m \cos(\omega_m n + \phi_m) \triangleq A_m \cos \Psi_m(n),$$

$x_{Q,m}(n) = A_m \sin(\omega_m n + \phi_m) \triangleq A_m \sin \Psi_m(n)$,

m : branch index = *1, 2, 3, ..., M,*

n : discrete time index,

A : amplitude,

ω : normalized frequency,

Ψ : random phase.

Also, referring to the notation in Fig. 3, the error signal e(n) is represented by

$$e(n) = \sum_{m=1}^{M} [c_{I,m}\ \tilde{e}_{I,m}(n) + c_{Q,m}\ \tilde{e}_{Q,m}(n)] + \eta(n)$$
$$= -\sum_{m=1}^{M} A_m [c_{I,m}\cos\Psi_m(n) + c_{Q,m}\sin\Psi_m(n)]\{w_{I,m}(n) - w_{I,m}^*\}$$
$$- \sum_{m=1}^{M} A_m [c_{I,m}\sin\Psi_m(n) - c_{Q,m}\cos\Psi_m(n)]\{w_{Q,m}(n) - w_{Q,m}^*\}$$
$$+ \eta(n) \qquad (2)$$

where

$$\tilde{e}_I(n) \triangleq \tilde{e}(n) = \sum_{m=1}^{M} \{ d_m(n) - y_m(n) \},$$

$\tilde{e}_Q(n)$: 90° phase-shifted version of $\tilde{e}_I(n)$

$\eta(n)$: zero-mean measurement noise.

Assuming that $\omega_{I,m}(n)$ and $\omega_{Q,m}(n)$ are slowly time-varying as compared to $x_{I,m}(n)$ and $x_{Q,m}(n)$, the phase-shifted output is giver from (1) by

$$y_Q(n) = \sum_{m=1}^{M} \{w_{I,m}(n)\, x_{Q,m}(n) - w_{Q,m}(n)\, x_{I,m}(n)\}$$
$$= \sum_{m=1}^{M} A_m \{w_{I,m}(n) \sin\Psi_m(n) - w_{Q,m}(n) \cos\Psi_m(n)\}. \qquad (3)$$

It can be shown from (1), (2) and (3) that minimizing the fourth power error and using a gradient-descent method yields[3] a pair of the filtered-x LMF weight update equations for each m as

$$w_{I,m}(n+1) = w_{I,m}(n) + 2\mu_m e^3(n)\{c_{I,m}x_{I,m}(n) + c_{Q,m}x_{Q,m}(n)\}$$
$$w_{Q,m}(n+1) = w_{Q,m}(n) + 2\mu_m e^3(n)\{c_{I,m}x_{Q,m}(n) - c_{Q,m}x_{I,m}(n)\} \qquad (4)$$

where μm is a convergence constant.

It is noted that to implement the filtered-x LMF algorithm of (4), the values of $c_{I,m}$ and $c_{Q,m}$ must be estimated. In the following, we analyze the effects of replacing $c_{I,m}$ and $c_{Q,m}$ in (4) with $\hat{c}_{I,m}$ and $\hat{c}_{Q,m}$ on the convergence behavior of the canceller.

In the following, we analyze the convergence behavior of the mean and summed variance of weight errors of the filtered-x LMF algorithm using a new analysis method.

Ⅲ. Convergence Analysis

A. The mean of weight error (Magnitude)

To see how the adaptive algorithm derived in (4) converges for inaccurate $\hat{c}_{I,m}$ an $\hat{c}_{Q,m}$, we first investigate the convergence of the expected values of the adaptive weights. To simplify the convergence equation, we may introduce two weight errors as

$$v_{I,m}(n) \triangleq w_{I,m}(n) - w_{I,m}^*,$$
$$v_{Q,m}(n) \triangleq w_{Q,m}(n) - w_{Q,m}^*. \qquad (5)$$

Then, from (2), (5) and Fig. 3, we get

$$\tilde{e}_{I,m}(n) = -v_{I,m}(n)\, x_{I,m}(n) - v_{Q,m}(n)\, x_{Q,m}(n),$$
$$\tilde{e}_{Q,m}(n) = -v_{I,m}(n)\, x_{Q,m}(n) + v_{Q,m}(n)\, x_{I,m}(n). \qquad (6)$$

Inserting (5) into (4), we have

$$v_{I,m}(n+1) = v_{I,m}(n) + 2\mu_m e^3(n)\{\hat{c}_{I,m}x_{I,m}(n) + \hat{c}_{Q,m}x_{Q,m}(n)\},$$
$$v_{Q,m}(n+1) = v_{Q,m}(n) + 2\mu_m e^3(n)\{\hat{c}_{I,m}x_{Q,m}(n) - \hat{c}_{Q,m}x_{I,m}(n)\}. \qquad (7)$$

Rearranging (7) with (2) and (6), taking expectation of both sides of the resultant two weight-error equations, we can get the convergence equation based on the independent assumption on the underlying signal ; $x_m(n)$, $\eta(n)$, $v_{I,m}(n)$ and $v_{Q,m}(n)$.

The moment terms of order greater than 1 decrease much faster than the first order moment term in $E[v_{I,m}(n)]$ and $E[v_{Q,m}(n)]$. Therefore, ignoring the moment terms of order greater than 1, the convergence equation becomes

$$\begin{bmatrix} E[v_{I,m}(n+1)] \\ E[v_{Q,m}(n+1)] \end{bmatrix} \cong \begin{bmatrix} \alpha_m & \beta_m \\ -\beta_m & \alpha_m \end{bmatrix} \begin{bmatrix} E[v_{I,m}(n)] \\ E[v_{Q,m}(n)] \end{bmatrix} \quad (8)$$

where

$\alpha_m \triangleq 1 - 3\mu_m A_m^2 g_m \hat{g}_m \sigma_\eta^2 \cos\triangle\theta_{c,m}$,,

$\beta_m \triangleq 3\mu_m A_m^2 g_m \hat{g}_m \sigma_\eta^2 \sin\triangle\theta_{c,m}$.

Here, defining gain and phase response parameters as

$g_m \triangleq \sqrt{c_{I,m}^2 + c_{Q,m}^2}$,

$\hat{g}_m \triangleq \sqrt{\hat{c}_{I,m}^{\ 2} + \hat{c}_{Q,m}^{\ 2}}$,

$\theta_{c,m} \triangleq \tan^{-1}\left(\frac{c_{Q,m}}{c_{I,m}}\right)$,

$\hat{\theta}_{c,m} \triangleq \tan^{-1}\left(\frac{\hat{c}_{Q,m}}{\hat{c}_{I,m}}\right)$,

$\triangle\theta_{c,m} \triangleq \theta_{c,m} - \hat{\theta}_{c,m}$.

Now, using the similarity transform to make $E[v_{I,m}(n)]$ and $E[v_{Q,m}(n)]$ in decoupled forms, (8) can be expressed as follows.

$$\begin{bmatrix} E[\breve{v}_{I,m}(n+1)] \\ E[\breve{v}_{Q,m}(n+1)] \end{bmatrix} = \begin{bmatrix} 1-\lambda_{I,m} & 0 \\ 0 & 1-\lambda_{Q,m} \end{bmatrix} \begin{bmatrix} E[\breve{v}_{I,m}(n)] \\ E[\breve{v}_{Q,m}(n)] \end{bmatrix} \quad (9)$$

where

$\lambda_{i,m} = 3\mu_m A_m^2 g_m \hat{g}_m \sigma_\eta^2 [\cos\triangle\theta_{c,m} \pm j\sin\triangle\theta_{c,m}]$, $i = I, Q$.

Since $\lambda_{i,m}$ in (9) is a complex number, the transformed weight error is also complex. When a complex number is given, we consider its real and imaginary parts individually or investigate the convergence of magnitude of transformed weight error.

$$|E[v_{i,m}(n+1)]| = |1-\lambda_{i,m}|\,|E[v_{i,m}(n)]|, \quad i = I, Q. \quad (10)$$

As it is clearly seen in(10), the magnitude of weight error converges exponentially to 0 under following conditions.

$$|1-\lambda_{i,m}| < 1 \quad \forall_{i,m}, \quad i = I, Q. \quad (11)$$

Squaring both sides of(11) and rearranging the terms, the stabilizing condition are obtained.

$$0 < \mu_m < \frac{2\cos\triangle\theta_{c,m}}{3A_m^2 g_m \hat{g}_m \sigma_\eta^2} \text{ or } 0 < \varkappa_{m,f} < 1 \quad (12)$$

where

$$\varkappa_{m,f} \triangleq \frac{3\mu_m A_m^2 g_m \hat{g}_m \sigma_\eta^2}{2\cos\triangle\theta_{c,m}}.$$

We see that stabilizing condition of (12), unlike the filtered-x LMS, is affected by variance of measurement noise signal[11~12]. In a sufficiently large time constant τ domain, time constant τ for exponential convergence can be simplified and is derived[3].

$$e^{-1/\tau_{i,m}} \cong 1 - \frac{1}{\tau_{i,m}} = |1-\lambda_{i,m}|, \quad i = I, Q. \quad (13)$$

From (10) and (13) the time constant is

$$\tau_i = \frac{1}{1-\sqrt{1-6\mu_m A_m^2 g_m \hat{g}_m \sigma_\eta^2 \cos\triangle\theta_{c,m} + 9\mu_m^2 A_m^4 g_m^2 \hat{g}_m^{\ 2} \sigma_\eta^4}}$$

$, i = I, Q$

$$= \frac{1}{1-\sqrt{1-4\varkappa_{m,f}(1-\varkappa_{m,f})\cos^2\triangle\theta_{c,m}}}. \quad (14)$$

B. Summed variance of weight errors

Next we investigate the convergence of the mean-square error (MSE), $E[e^2(n)]$. Using (2) and (6), we can express the MSE as

$$E[e^2(n)] = \sum_{m=1}^{M} e_m^2(n) + \sigma_\eta^2 = \frac{1}{2}\sum_{m=1}^{M} A_m^2 \xi_m(n) + \sigma_\eta^2 \quad (15)$$

where

$\xi_m(n) \triangleq E[v_{I,m}^2(n)] + E[v_{Q,m}^2(n)]$,

$\sigma_\eta^2 \triangleq E[\eta^2(n)]$.

From (15), we find that studying the convergence of MSE is directly related to studying the sum of $\xi_m(n)$. Inserting (1) and (2) into (5), and assuming that input signal $x_m(n)$, measurement noise $\eta(n)$, and weight errors $v_{I,m}(n)$, $v_{Q,m}(n)$ are independent of each other, we take the statistical average of both sides to

obtain two equations for $E[v_I^2(n+1)]$, $E[v_Q^2(n+1)]$. Since there two equations are symmetrical, we add them and assume that $E[v_{I,m}^2(n+1)] \cong E[v_{Q,m}^2(n+1)]$. Thus, eliminating the subscripts I and Q to simplify the second moment equation of weight error and rearranging the terms yields

$$
\begin{aligned}
&E[v_m^2(n+1)] \\
&= \frac{5}{4}\mu_m^2 A_m^8 g_m^6 \ \hat{g}_m^{\ 2}\{E[v_m^6(n)]+3E[v_m^2(n)]E[v_m^4(n)]\} \\
&-\frac{3}{2}\mu_m A_m^4 g_m^3 \hat{g}_m \cos\triangle\theta_{c,m}\{E[v_m^4(n)]+(E[v_m^2(n)])^2\} \\
&+\frac{45}{2}\mu_m^2 A_m^6 g_m^4 \ \hat{g}_m^{\ 2} E[\eta^2(n)]\{E[v_m^4(n)]+(E[v_m^2(n)])^2\} \\
&+\{1-6\mu_m A_m^2 g_m \hat{g}_m E[\eta^2(n)]\cos\triangle\theta_{c,m} \\
&+30\mu_m^2 A_m^4 g_m^2 \ \hat{g}_m^{\ 2} E[\eta^4(n)]\} E[v_m^2(n)] \\
&+2\mu_m^2 A_m^2 \ \hat{g}_m^{\ 2} E[\eta^6(n)]. \qquad (16)
\end{aligned}
$$

Assuming that $\eta(n)$ is a Gaussian with zero average and $\omega_{I,m}(n)$, $\omega_{Q,m}(n)$ are Gaussian variables, $v_m(n)$ is also a Gaussian variable. Thus, (16) can be simplified by expressing $E[v_m^{2K}(n)]$ as $E[v_m^2(n)]$ Although $E[v_m(n)]$ decreases very rapidly, it is no zero from the beginning. Thus, a Gaussian random variable $\triangle w_m(n)$ with zero average, and its variance are adapted as follows:

$$
\begin{aligned}
&\triangle w_m(n) \triangleq v_m(n) - V_m(n), \\
&E[v_m^2(n)] = V_m^2(n) + \rho_m^2(n) \qquad (17)
\end{aligned}
$$

where $V_m(n) \triangleq E[v_m(n)]$,

$\rho_m^2(n) \triangleq E[\triangle^2 w_m(n)]$.

From (17), we find that during the transient state, i.e. from beginning to the moment just before the steady state, $\rho_m^2(n)$ is much smaller than $V_m^2(n)$ and $E[v_m(n)]$ can be regarded as $V_m^2(n)$. On the other hand, $\rho_m^2(n)$ becomes dominant over $V_m^2(n)$ in the steady state and $E[v_m(n)]$ can be regarded as $\rho_m^2(n)$. Now, we apply (17) to (16) and use the relationship between $E[v_m^{2K}(n)]$ and $E[v_m^2(n)]$ of the Gaussian random variable[13] to arrive at the following equation.

$$
\begin{aligned}
&V_m^2(n+1)+\rho_m^2(n+1) \\
&=5\mu_m^2 A_m^8 g_m^6 \ \hat{g}_m^{\ 2}\{V_m^6(n)+9\rho_m^2(n)V_m^4(n) \\
&+18\rho_m^4(n)V_m^2(n)+6\rho_m^6(n)\} \\
&-(3\mu_m A_m^4 g_m^3 \hat{g}_m \cos\triangle\theta_{c,m}-45\mu_m^2 A_m^6 g_m^4 \ \hat{g}_m^{\ 2}\sigma_\eta^2) \\
&\cdot\{V_m^4(n)+4\rho_m^2(n)V_m^2(n)+2\rho_m^4(n)\} \\
&+(1-6\mu_m A_m^2 g_m \hat{g}_m \sigma_\eta^2 \cos\triangle\theta_{c,m}+90\mu_m^2 A_m^4 g_m^2 \ \hat{g}_m^{\ 2}\sigma_\eta^4) \\
&\cdot\{V_m^2(n)+\rho_m^2(n)\} \\
&+30\mu_m^2 A_m^2 \ \hat{g}_m^{\ 2}\sigma_\eta^6. \qquad (18)
\end{aligned}
$$

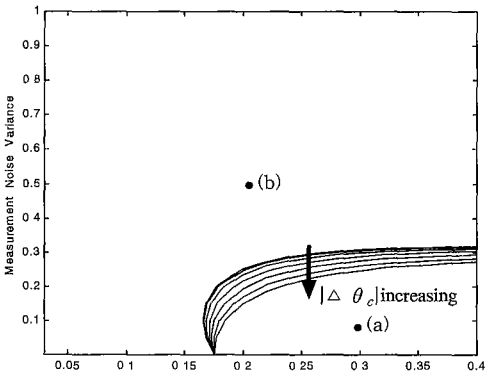

Fig. 4 Dominant term decision diagram for filtered-x LMF algorithm of summed variance of weight errors at the transient-state.
[point (a) : $\mu_m=0.3$ and $\sigma_\eta^2=0.1$. point (b) : $\mu_m=0.2$ and $\sigma_\eta^2=0.5$.]

(1) Convergence during the transient state

The convergence equation (18) may be examined for two different cases. First, $\rho_m^{2K}(n)$ and the last term of (18) can be removed for the transient state. Thus, the transient convergence equation is given by

$$
\begin{aligned}
&V_m^2(n+1) \cong 5\mu_m^2 A_m^8 g_m^6 \ \hat{g}_m^{\ 2} V_m^6(n) \\
&-(3\mu_m A_m^4 g_m^3 \hat{g}_m \cos\triangle\theta_{c,m}-45\mu_m^2 A_m^6 g_m^4 \ \hat{g}_m^{\ 2}\sigma_\eta^2) V_m^4(n) \\
&+(1-6\mu_m A_m^2 g_m \hat{g}_m \sigma_\eta^2 \cos\triangle\theta_{c,m}+90\mu_m^2 A_m^4 g_m^2 \ \hat{g}_m^{\ 2}\sigma_\eta^4) V_m^2(n) \\
&\qquad (19)
\end{aligned}
$$

On the right side of (19), either $V_m^6(n)$ or $V_m^2(n)$ becomes a dominant term in extreme cases. When the two terms have same values, we can write $V_m^2(n)$ as follow

$$V_{m,th}^2 = \sqrt{\frac{1-6\mu_m A_m^2 g_m \hat{g}_m \sigma_\eta^2 \cos\triangle\theta_{c,m} + 90\mu_m^2 A_m^4 g_m^2 \hat{g}_m^2 \sigma_\eta^4}{5\mu_m^2 A_m^8 g_m^6 \hat{g}_m^2}}. \tag{20}$$

Note that $\triangle\theta_{c,m}$ does not affect $V_{m,th}^2$. In (19), the first term $V_m^6(n)$ acts as the dominant term when $V_m^2(n)$ is greater than $V_{m,th}^2$. If V_m^2 is smaller than $V_{m,th}^2$, then the last $V_m^6(n)$ term becomes dominant. Fig. 4 is given to illustrate in terms of the convergence constant μm and the variance of measurement noise σ_η^2, which of the two terms, the first term $V_m^6(n)$ and the last term $V_m^2(n)$, is dominant when $V_{m,th}^2(n)$ = 0.8. Point (a) is a region in which the term $V_m^6(n)$ dominates over the other and point (b) is when $V_m^2(n)$ term is the dominant one. Therefore, the transient convergence equation (19) can be written as:

$$V_m^2(n+1) \cong \begin{cases} 5\mu_m^2 A_m^8 g_m^6 \hat{g}_m^2 V_m^6(n) & , V_m^2(n) \gg V_{m,th}^2 \quad (21a) \\ (1-6\mu_m A_m^2 g_m \hat{g}_m \sigma_\eta^2 \cos\triangle\theta_{c,m} & \\ \quad +90\mu_m^2 A_m^4 g_m^2 \hat{g}_m^2 \sigma_\eta^4) V_m^2(n) & , V_m^2(n) \ll V_{m,th}^2. \quad (21b) \end{cases}$$

Now, from (21a) we may derive the conditions for stability and the time constant by rewriting it as

$$\begin{aligned} V_m^2(n) &= \{5\mu_m^2 A_m^8 g_m^6 \hat{g}_m^2\}^{(3^n-1)/2} \{V_m^2(0)\}^{3^n} \\ &= \frac{1}{\sqrt{5}\mu_m A_m^4 g_m^3 \hat{g}_m} \{\sqrt{5}\mu_m A_m^4 g_m^3 \hat{g}_m V_m^2(0)\}^{3^n}. \end{aligned} \tag{22}$$

Thus, (22) is stable under the following condition:

$$\begin{aligned} &|\sqrt{5}\mu_m A_m^4 g_m^3 \hat{g}_m V_m^2(0)| < 1, \\ &0 < \mu_m < \frac{1}{\sqrt{5} A_m^4 g_m^3 \hat{g}_m V_m^2(0)}. \end{aligned} \tag{23}$$

Note from the conditions for stability in (23) that the initial value of weight error acts as a limiting factor, along with the amplitude of input signal, the gain of the secondary path and the estimated gain of the secondary path. And, (21b) is stabilized when it satisfies the condition below;

$$0 < \mu_m < \frac{\cos\triangle\theta_{c,m}}{15 A_m^2 g_m \hat{g}_m \sigma_\eta^2} \text{ or } 0 < \chi_{m,s} < 1 \tag{24}$$

where

$$\chi_{m,s} \triangleq \frac{15\mu_{Fx,m} A_m^2 g_m \hat{g}_m \sigma_\eta^2}{\cos\triangle\theta_{c,m}}.$$

From (13) and (21b), the time constant is given by;

$$\begin{aligned} \tau_{m,s} &= \frac{1}{6\mu_m A_m^2 g_m \hat{g}_m \sigma_\eta^2 \{\cos\triangle\theta_{c,m} - 15\mu_m A_m^2 g_m \hat{g}_m \sigma_\eta^2\}} \\ &= \frac{5}{2\chi_{m,s}\cos^2\triangle\theta_{c,m}\{1-\chi_{m,s}\}}. \end{aligned} \tag{25}$$

(2) Convergence in the steady state

In the steady state, $V_m^2(n)$ becomes sufficiently small and the terms that include $\rho_m^4(n)$ and $\rho_m^6(n)$ can be ignored in the convergence equation (18). The equation is then simplified as

$$\begin{aligned} \rho_m^2(n+1) \cong (1 &- 6\mu_m A_m^2 g_m \hat{g}_m \sigma_\eta^2 \cos\triangle\theta_{c,m} \\ &+ 90\mu_m^2 A_m^4 g_m^2 \hat{g}_m^2 \sigma_\eta^4) \rho_m^2(n) \\ &+ 30\mu_m^2 A_m^2 \hat{g}_m^2 \sigma_\eta^6. \end{aligned} \tag{26}$$

And, the summed variance of weight errors in the steady state, $\xi_m(\infty)$ is $2\rho_m(\infty)$ and it can be written as

$$\begin{aligned} \xi_m(\infty) = 2\rho_m(\infty) &= \frac{10\mu_m \hat{g}_m \sigma_\eta^4}{g_m\{\cos\triangle\theta_{c,m} - 15\mu_m A_m^2 g_m \hat{g}_m \sigma_\eta^2\}} \\ &= \frac{2\sigma_\eta^2 \chi_{m,s}}{3A_m^2 g_m^2 \{1-\chi_{m,s}\}}. \end{aligned} \tag{27}$$

(3) Comparison of the filtered-x LMF (FXLMF) and filtered-x LMS(FXLMS) algorithm

Comparing the performance of adaptive algorithms usually involves two methods. The first method is to compare the state of convergence after setting equal values for the steady state, and the other one involves

comparing the steady state values for same rate of convergence.

Like (18) in [12] the summed variance of weight errors of the FXLMS algorithm is a geometric series and the time constant can be defined while that of the FXLMF algorithm (18) is not a geometric series and therefore, the time constant may not be defined. Then we set the steady state values of the two algorithms equal and compare the convergence rates. From (27) and (20) in [12] we obtain following equation.

$$\frac{10\mu_{m(FXLMF)}\,\hat{g}_m\,\sigma_\eta^4}{g_m\{\cos\triangle\theta_{c,m}-15\mu_{m(FXLMF)}A_m^2 g_m\,\hat{g}_m\,\sigma_\eta^2\}} = \frac{\mu_{m(FXLMS)}\,\hat{g}_m\,\sigma_\eta^2}{g_m\{\cos\triangle\theta_{c,m}-\frac{1}{16}\mu_{m(FXLMS)}A_m^2 g_m\,\hat{g}_m(9-\cos 2\triangle\theta_{c,m})\}}. \tag{28}$$

where $\mu_{m(FXLMF)}$ and $\mu_{m(FXLMS)}$ are the convergence constants of FXLMF and FXLMS algorithms, respectively.

When the convergence constants $\mu_{m(FXLMF)}$ and $\mu_{m(FXLMS)}$ satisfy the stability conditions, the second terms on both sides of (28) are sufficiently smaller than the first terms and they are ignored to yield the following equation.

$$\mu_{m(FXLMF)} = \frac{\mu_{m(FXLMS)}}{10\,\sigma_\eta^2}. \tag{29}$$

Ⅳ. Computer Simulations

In this section, we present the results obtained from computer simulation along with the theoretical analysis of FXLMF algorithm in the previous section.

We set the frequencies of the first and second sinusoidal signal at 120 Hz and 240 Hz, respectively, and selected 2 KHz for sampling frequency. The input signal $x(n)$ and desired signal $d(n)$ are given by

$$x(n) = \sum_{m=1}^{2} A_m \cos(\omega_m n + \phi_m)$$

$$= \sqrt{2}\{\cos(\frac{240\pi n}{2000} + \phi_1) + \cos(\frac{480\pi n}{2000} + \phi_2)\},$$

$$d(n) = \sum_{m=1}^{2}\{w_{I,m}^* x_{I,m} + w_{Q,m}^* x_{Q,m}\}$$

$$= 0.6\,x_{I,1}(n) - 0.1\,x_{Q,1}(n) + 0.3\,x_{I,2}(n) - 0.3\,x_{Q,2}(n). \tag{30}$$

The secondary path is modeled as $g_1 = g_2 = 1$, $\theta_{c,1} = -45^\circ$ and $\theta_{c,2} = 45^\circ$. The simulation was carried out by setting 0.001 and 1 as the variances of measurement noise σ_η^2. And the initial value of weights is zero. The simulation averaging 1000 independent runs.

Fig. 5. showed the summed variance convergence curve of weight error for the FXLMF algorithm that resulted from the simulation when $\mu_{1(FXLMF)} = 0.2$, $\sigma_\eta^2 = 0.001$, and $|\triangle\theta_{c,1}| = 15^\circ$. We see that $V^2(n)$ is the dominant term during the transient state whereas $\rho^2(n)$ becomes dominant during the steady state.

Fig. 6. showed the summed variance convergence curve of weight error that resulted from the simulation when the phase estimation error $|\triangle\theta_{c,m}|$ is (1) 0° , (2) 45° , (3) 60° , (4) 75° under the same value in the steady state. It can be seen that the larger phase estimation error is, the slower the convergence speed is, and that the steady-state value is not affected by the phase estimation error $|\triangle\theta_{c,m}|$

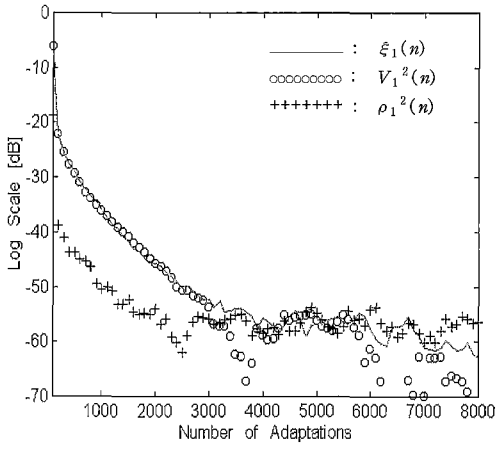

Fig. 5 Learning curves for filtered-x LMF algorithm of summed variance of weight errors when the convergence behavior are divided between $V_2(n)$ and $\rho^2(n)$
[$\mu_{1(FXLMF)} = 0.2$, σ_η^2=0.001, and $|\triangle\theta_{c,1}| = 15^\circ$]]

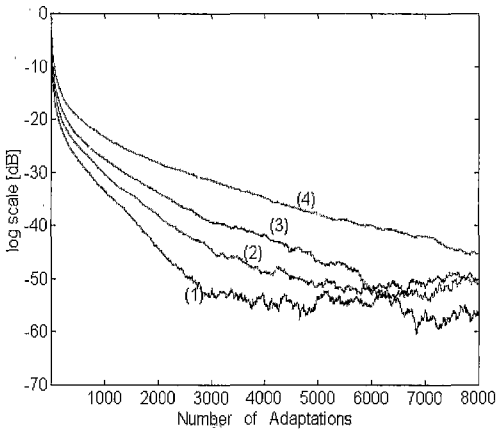

Fig. 6 Learning curves for filtered-x LMF algorithm of summed variance of weight errors. [$\mu_{1(FXLMF)} = 0.2$ and $\sigma_\eta^2 = 0.001$] (1) $|\triangle\theta_{c,m}| = 0°$. (2) $|\triangle\theta_{c,m}| = 45°$. (3) $|\triangle\theta_{c,m}| = 60°$. (4) $|\triangle\theta_{c,m}| = 75°$

We have compared the convergence behavior of FXLMF algorithm and that of algorithm FXLMS through simulation. The convergence speed of the two algorithm were compared after setting the steady-state values equal. The convergence constants of FXLMF and FXLMS algorithm were carefully chosen so that they satisfy the conditions given in (29) for a given variance of measurement signal. To be specific, we selected 0.2 and 0.0002 for $\mu_{(FXLMF)}$ to make the steady-state values of two algorithm equal when σ_η^2 is given as 0.001 and 1 and $\mu_{(FXLMS)}$ is 0.002.

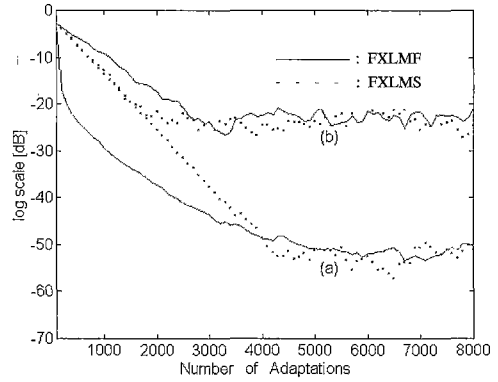

Fig. 7 Comparison of the FXLMS and FXLMF algorithm learning curves of the summed variance of weight errors.
(a) $\mu_{(FXLMS)} = 0.002$, $\mu_{(FXLMF)} = 0.2$,,
$\sigma_\eta^2 = 0.001$, $|\triangle\theta_{c,m}| = 45°$ and $V_{th}^2 = 0.558$
(b) $\mu_{(FXLMS)} = 0.002$, $\mu_{(FXLMF)} = 0.0002$,
$\sigma_\eta^2 = 1$, $|\triangle\theta_{c,m}| = 45°$, and $V_{th}^2 = 558$.

In Fig. 7, the convergence behavior curves of summed variance of weight error obtained from simulation are compared with each other when the phase estimation error $|\triangle\theta_{c,m}|$ is 45° . It has been newly found that for some region of μ and σ_η^2, resulting in sufficiently small V_{th}^2 values compared to unity as the curve (a) of Fig. 7, the initial convergence of the FXLMF algorithm is much faster than the conventional FXLMS algorithm. Later on, the FXLMF convergence looks similar to the FXLMS case. On the other hand, when V_{th}^2 is large as the curve (b) of Fig. 7, the FXLMF algorithm converges geometrically at a rate a bit slower than the FXLMS case.

V. Conclusions

The convergence result of the filtered-x LMF algorithm indicates that the effects of the parameter estimation inaccuracy on the convergence behavior of the algorithm are characterized by two distinct components: Phase estimation error and estimated gain. In particular, the convergence has been shown to be strongly affected by the accuracy of the phase response estimate. Also, it has been found that the mean square convergence behavior can differ depending on the power of Gaussian measurement noise and the size of convergence constants. Accordingly, the transient behavior can be characterized by one of the two cases: (1) initially, the filtered-x LMF algorithm converges much faster than the filtered-x LMS, but soon after that, it converges almost linearly on logarithmic scale like the filtered-x LMS algorithm; (2) the filtered-x LMF algorithm converges linearly and at a slower rate than the filtered-x LMS. To sum up, different convergence behavior was observed depending on the variance of Gaussian measurement noise and the magnitude of convergence constant.

References

[1] S. J. Elliott and P. A. Nelson, "The Active Control of Sound," Jour. Electronics and

Communication Eng., pp. 127-136, 1990.

[2] R. R. Leitch and M. O. Tokhi, "Active Noise Control Systems, "*Proc. IEE*, Vol. 134, Pt. A, No. 6, pp. 525-546, 1987.

[3] B. Widrow and S. D. Stearns, *Adaptive Signal Processing : Prentice-Hall*, 1985.

[4] J. C. Burgess, "Active Adaptive Sound Control in a Duct: A Computer Simulation," *Jour. Acoust. Soc. Am.*, Vol. 70, No. 3, pp. 715-726, 1981.

[5] D. Duttweiler, "Avoiding Slow Band-Edge Convergence in Subband Echo Cancelers," *IEEE Trans. on Signal Processing*, Vol. 49, No. 3, pp. 593-603, 2001.

[6] E. Walach and B. Widrow, "The Least Mean Fourth (LMF) Adaptive Algorithm and Its Family," *IEEE Trans. on Information Theory*, Vol. 30, No. 2, pp. 275-283, March 1984.

[7] A. Zerguin and T. Aboulnasr, "Convergence Behavior of the Normalized Least Mean Fourth Algorithm," *2000 International Conference on Acoustics, Speech, and Signal Processing*, Vol. I, pp. 279-282, 2000

[8] S. J. Elliott, I. M. Stothers and P. A. Nelson, "A Multiple Error LMS Algorithm and Its Application to the Active Control of Sound and Vibration," *IEEE Trans. on Acoustics, Speech and Signal Processing*, Vol. 35, No. 10, pp. 1423-1434, October 1987.

[9] A. Wang and W. Ren, "Convergence Anaysis of the Multi-Variable Filtered-X LMS Algorithm with Application to Active Noise Control," *IEEE Trans. on Signal Processing*, Vol. 47, No. 4, pp. 1166-1169, April, 1999

[10] S. Kuo, M. Tahernezhadi, and W. Hao "Convergence Anaysis of Narrow-Band Active Noise Control System," *IEEE Trans. on Circuits and Systems-II*, Vol. 46, No. 2, pp. 220-223, February, 1999

[11] K. S. Lee, J. C. Lee, D. H. Youn and I. W. Cha, "Convergence Analysis of the Filtered-x LMS Active Noise Canceller for a Sinusoidal Input," *Fifth Western Pacific Regional Acoustic Conference*, Vol. 2, pp. 873-878, August 23-25 1994

[12] K. S. Lee, J. C. Lee and D. H. Youn, "On the Convergence Behavior of the Filtered-xLMS Active Noise Canceler," *IEEE International Workshop on Intelligent Signal Processing and Communication Systems*, October 5-7, 1994.

[13] J. S. Bendat, *Nonlinear System Analysis and Identification from Random Data : John Wiley & Sons*, 1990.

Kang Seung Lee was bone in Korea, in 1962.

He received the B.S., M.S., and Ph.D. degree in electronic engineering from Yonsei University, Seoul, Korea, in 1985, 1991 and 1995, respectively.

From 1991 to 1995, he served as a Research Associate at Yonsei University. From 1987 to 1996, he served as a Senior Member of Research Staff at Korea Electric Power Research Center, Taejeon City. Since 1996, he has been with the Department of Computer Engineering, Dongeui University, Pusan, as an Assistant Professor. He also held visiting appointment with the Electrical Engineering Department at Stanford University from 2000 to 2001. His research interests include adaptive digital signal processing, image processing, multimedia signal processing and digital communications.

He is a member of IEEE(the Institute of Electrical and Electronics Engineers), AES(Audio Engineering Society), the Korea Institute of Telematics and Electronics, the Korean Institute of Communication Sciences, and the Acoustical Society of Korea.